Progress In Electromagnetics Research B, Vol. 23, 229–249, 2010

PHOTONIC BAND STRUCTURE OF 1D PERIODIC COMPOSITE SYSTEM WITH LEFT HANDED AND RIGHT HANDED MATERIALS BY GREEN FUNCTION APPROACH

A. Essadqui, J. Ben-Ali, and D. Bria †

Laboratoire de Dynamique et d'Optique des Matériaux
Faculté des Sciences
Université Mohamed I
60000 Oujda, Morocco

B. Djafari-Rouhani

Institut d'Electronique, de Microélectronique et de Nanotechnologie (IEMN)
UMR CNRS 8520
Université de Lille1
59655 Villeneuve d'Ascq Cedex, France

A. Nougaoui

Laboratoire de Dynamique et d'Optique des Matériaux
Faculté des Sciences
Université Mohamed I
60000 Oujda, Morocco

Abstract—In the framework of the Green function method, we theoretically study the photonic band structure of one-dimensional superlattice composed of alternating layers of right-handed and left-handed materials (RHM and LHM). The dispersion curves are studied by assuming that the dielectric permittivity and magnetic permeability are frequency dependent in each layer. It is shown that such structures can exhibit new types of electromagnetic modes and dispersion curves that do not exist in usual superlattices composed only of RHM.

Received 24 March 2010, Accepted 16 July 2010, Scheduled 23 July 2010
Corresponding author: D. Bria (bria@fso.ump.ma).
† D. Bria is also with Institut d'Electronique, de Microélectronique et de Nanotechnologie (IEMN), UMR CNRS 8520, Université de Lille1, 59655 Villeneuve d'Ascq Cedex, France; The Abdus Salam International Centre for Theoretical Physics, Trieste, Italy.

With an appropriate choice of the parameters, we show that it is possible to realize an absolute (or omnidirectional) band gap for either transverse electric (TE) or transverse magnetic (TM) polarizations of the electromagnetic waves. A combination of two multilayer structures composed of RHM and LHM is proposed to realize, in a certain range of frequency, an omnidirectional reflector of light for both polarizations.

1. INTRODUCTION

Left handed materials (LHM), in which the dielectric permittivity ε and magnetic permeability μ are simultaneously negative, have received a great deal of attention during the last few years [1]. This is due to the unusual physical properties of these materials that have raised strong theoretical interest and may lead to potential applications in optical devices. Some peculiar properties of LHM have already been discussed some thirty years ago by Veselago [2] for instance a negative index of refraction in such a medium, a Poynting vector directed opposite to the propagation wave vector $\mathbf{k}$, the reversal of Doppler and Cerenkov effects. Because of the absence of naturally existing LHM, the experimental realization of an artificial heterogeneous medium exhibiting a negative index of refraction has been performed only recently [3]. The realization of such media [3, 4] is based on the propositions of Pendry et al. for specific structures exhibiting negative $\varepsilon(\omega)$ and $\mu(\omega)$ [5]. Recent interest in these metamaterials has been directed towards the theoretical and experimental study of Snell's law of refraction at the boundary with a LHM [6–10], the focusing and imaging properties of a metamaterial lens [11–13], the tunnelling in the presence of a LHM layer [14], the emission in a LHM metamaterial [15], etc.

Assuming the possibility of realizing such LHM under the form of layered media, a few recent works have investigated the photonic band structure of one dimensional layered structures constituted by a periodical repetition of RHM and LHM [16–24]. Some peculiar properties related to the presence of LHM layers have been underlined, for instance the possibility of gap widening with respect to usual superlattices constituted only by RHM [16], the theoretical and experimental investigation of a new type of gap when the average index of refraction in the superlattice vanishes [17] and the possibility of discrete and photon tunnelling modes [19]. These works have mainly concentrated on propagation along the axis of the superlattice, i.e., normal incidence.

The object of this paper is to present theoretically a detailed study of the dispersion relation and photonic band structure in superlattices

constituted by alternate layers of LHM and RHM, with the aim of giving the different trends that can occur and emphasizing the new behaviors that have not been predicted before. We present and discuss the band structure with various physical parameters of the LHM layer. In these calculations, the dielectric permittivity ε and magnetic permeability μ are frequency dependent. We discuss, in particular, the photonic bands of the superlattice originating from the interface modes at the boundary between a RHM and a LHM, and those bands that are confined in one type of layer in the superlattice. We also show that for some particular choices of the physical and geometrical parameters, the RHM-LHM superlattice can exhibit an absolute (or omnidirectional) band gap for either TE or TM polarization of the electromagnetic field. This situation is without analogue in the case of usual superlattices. Thus, a combination in tandem of two LHM-RHM superlattices enables us to propose an omnidirectional reflector structure for both polarizations of the light. We note that the search of omnidirectional reflection gaps has been the object of several recent works [16, 25–30].

The confined modes of finite LHM layer embedded between two infinite RHM as well as the dispersion relation for infinite superlattice composed of LHM and RHM can actually be derived by using either the transfer matrix or the Green-function methods. This last one enable to investigate other vibrational properties of semi-infinte or finite superlattices such as the local and total densities of states, and therefore the spatial distribution of the states and, in particular, the possibility of resonant waves. We present in this paper explicit expressions of the Green function in these heterostructures. The knowledge of this Green's function enables us also to obtain the reflection and transmission coefficients of optical waves in one-dimensional heterostructure systems [27, 28].

The model and method of calculation are presented in Section 2. Section 3 contains the numerical illustrations as well as the discussion of the dispersion curves. Finally in Section 4, we propose a new solution to create complete gap for both wave polarizations in the one dimensional photonic crystal by the association of two semi infinite superlattices composed by LHM-RHM. Conclusion is given in Section 5.

2. MODEL AND THEORY ANALYSIS

2.1. Green Function Approach

We first consider a semi-infinite homogeneous medium (i) of relative dielectric permittivity ε_i and magnetic permeability μ_i, separated from

vacuum by a surface defined by the equation $z = f(x,y)$. The electric and magnetic fields at the interface can be related by Maxwell's equations:

$$\frac{1}{\varepsilon_i}\theta(z-f(x,y))\vec{\nabla}\wedge\vec{H} = \frac{\partial\vec{E}}{\partial t} \tag{1}$$

$$\frac{1}{\mu_i}\theta(z-f(x,y))\vec{\nabla}\wedge\vec{E} = -\frac{\partial\vec{H}}{\partial t} \tag{2}$$

where $\theta(z-f(x,y)) = \begin{cases} 1, & \text{for } z \geq f(x,y) \\ 0, & \text{for } z < f(x,y) \end{cases}$.

Taking the planar surface at $z = f(x,y) = 0$ and applying the nabla operator, we find

$$\vec{\nabla}\wedge(2) \Rightarrow \frac{1}{\mu_i}\left[\vec{\nabla}\theta(z)\wedge\vec{\nabla}\wedge\vec{E}+\theta(z)\wedge\vec{\nabla}\wedge\vec{E}\right]$$

$$= -\frac{\partial}{\partial t}\vec{\nabla}\wedge\vec{H} = -\theta(z)\varepsilon_i\frac{\partial^2\vec{E}}{\partial t^2} \tag{3}$$

$$\frac{1}{\mu_i}\theta(z)\left[\vec{\nabla}\wedge\vec{\nabla}\wedge\vec{E}+\varepsilon_i\mu_i\frac{\partial^2\vec{E}}{\partial t^2}\right]+\frac{1}{\mu_i}\vec{\nabla}(\theta(z))\wedge\vec{\nabla}\wedge\vec{E}=0 \tag{4}$$

where

$$\vec{\nabla}\theta(z)\wedge\vec{\nabla}\wedge\vec{E} = -\delta(z-f(x,y))\vec{V}_i(k_{//}/z)\vec{E} \tag{5}$$

$$\frac{1}{\mu_i}\theta(z)\left[\vec{\nabla}\wedge\vec{\nabla}\wedge\vec{E}+\varepsilon_i\mu_i\frac{\partial^2\vec{E}}{\partial t^2}\right]-\frac{1}{\mu_i}\delta(z-f(x,y))\vec{V}_i(k_{//}/z)\vec{E}=0 \tag{6}$$

We use the Fourier transformation ($t \to \omega$), and we define the response functions $\overleftrightarrow{G}_i(\omega/\vec{r},\vec{r}\,')$ and $\overleftrightarrow{g}_{si}(\omega/\vec{r},\vec{r}\,')$ respectively for infinite and semi-infinite system as:

$$\frac{1}{\mu_i}\left[\frac{\omega^2}{c^2}\varepsilon_i\mu_i - \overleftrightarrow{H}^0(k_{//}/z)\right]\overleftrightarrow{G}_i(\omega/\vec{r},\vec{r}\,') = \overleftrightarrow{I}\delta(\vec{r}-\vec{r}\,') \tag{7}$$

c is the speed of light in vacuum, ε_i and μ_i are the relative dielectric permittivity and magnetic permeability of the material, and the index of refraction is defined by $n_i = \pm\sqrt{\varepsilon_i\mu_i}$ with the plus or minus sign being used, respectively, for RHM and LHM. We assume that the z-axis is along the normal to the interface, and the wave vector component $k_{||}$, parallel to the interface, is along the x-axis.

$$\frac{1}{\mu_i}\left\{\theta(z)\left[\frac{\omega^2}{c^2}\varepsilon_i\mu_i-\overleftrightarrow{H}^0(k_{//}/z)\right]+\delta(z)\overleftrightarrow{V}_i\right\}\overleftrightarrow{g}_{si}(\omega/z,z')=\overleftrightarrow{I}\delta(z-z') \tag{8a}$$

where

$$\overleftrightarrow{H}^{0}(k_{||}/z) = \begin{pmatrix} -\frac{\partial^2}{\partial z^2} & 0 & ik_{||}\frac{\partial}{\partial z} \\ 0 & k_{||}^2 - \frac{\partial^2}{\partial z^2} & 0 \\ ik_{||}\frac{\partial}{\partial z} & 0 & k_{||} \end{pmatrix}$$

$$\text{and} \quad \overleftrightarrow{V}_{/}(k_{||}/z) = \begin{pmatrix} \frac{\partial}{\partial z} & 0 & ik_{||} \\ 0 & \frac{\partial}{\partial z} & 0 \\ 0 & 0 & 0 \end{pmatrix};\ z \geq 0 \tag{8b}$$

The determination of the matrix elements of $\overleftrightarrow{G}_i$ is greatly simplified by the fact that $(\overleftrightarrow{G}_i)_{21}$ and $(\overleftrightarrow{G}_i)_{32}$ satisfy homogenous equations. These four matrix elements therefore vanish in $\overleftrightarrow{G}_i$ and also in $\overleftrightarrow{g}_{si}$, and the 2×2 matrix elements decouple from the others. We can regard in what follows g_{11} and g_{22} as the primary elements of $\overleftrightarrow{g}_{si}$ and g_{31} and g_{33} as derived elements through Eq. (8). Eq. (8) can be rewritten as three independent equations for the 22, 11 and 13 elements $\overleftrightarrow{g}_{si}$, namely:

$$\frac{1}{\mu_i}\left\{\theta(z)\left(\frac{\partial^2}{\partial z^2} - \alpha_i^2\right) + \delta(z)\frac{\partial}{\partial z}\right\}(g_{si})_{22} = \delta(z - z') \tag{9a}$$

$$-\frac{\omega^2\varepsilon_i}{\alpha_i^2 c^2}\left\{\theta(z)\left(\frac{\partial^2}{\partial z^2} - \alpha_i^2\right) + \delta(z)\frac{\partial}{\partial z}\right\}(g_{si})_{11} = \delta(z - z') \tag{9b}$$

$$-\frac{\omega^2\varepsilon_i}{\alpha_i^2 c^2}\left\{\theta(z)\left(\frac{\partial^2}{\partial z^2} - \alpha_i^2\right)\right\}(g_{si})_{13}$$

$$-\delta(z)\left\{\delta(z - z') + \frac{i\omega^2\varepsilon_i}{k_{//}c^2}\frac{\partial}{\partial z}(g_{si})_{13}\right\} = \frac{\partial}{\partial z}\delta(z - z') \tag{9c}$$

So considering Eq. (9), one sees that all three are isomorphic to the same basic equation:

$$\frac{F_i}{\alpha_i}\left\{\theta(z)\left[-\alpha_i^2 + \frac{\partial^2}{\partial z^2}\right] + \delta(z)\frac{\partial}{\partial z}\right\} g_{si}(z, z') = \delta(z - z') \tag{10a}$$

where $\alpha_i^2 = k_{//}^2 - \frac{\omega^2}{c^2}\varepsilon_i\mu_i$ and

$$F_i = \frac{\alpha_i}{\mu_i} \text{ for } g_{22} \text{ (TE wave)}; \tag{10b}$$

$$F_i = -\frac{\varepsilon_i}{\alpha_i}\frac{\omega^2}{c^2} \text{ for } g_{11}(\text{TM wave}). \tag{10c}$$

So, it is sufficient to obtain the basic element of the response function g, starting with Eq. (10). The g_{13}, g_{31} and g_{33} are then easily obtained with the help of the equations following Eq. (8).

In our work, we have studied the optical waves in lamellar periodic structures in the framework of a Green's function method called also the interface response theory [31]. The object of this theory is to calculate the Green's function of a composite system containing a large number of interfaces that separate different homogeneous media. In this theory the Green's function of a composite system can be written as [31, 32]

$$\begin{aligned} g(DD) \;=\; & G(DD) + G(DM)\{[G(MM)]^{-1} g(MM) \\ & [G(MM)]^{-1}[G(MM)]^{-1}\} G(MD) \end{aligned} \tag{11}$$

where D and M are respectively the whole space and the space of the interfaces in the lamellar system. G is a block-diagonal matrix in which each block G_i corresponds to the bulk Green's function of the subsystem i. All the matrix elements $g(DD)$ of the composite material can be obtained from the knowledge of the matrix elements $g(MM)$ of g in the interface space M. The $g(MM)$ is calculated by inverting the matrix $g^{-1}(MM)$ formed by a linear superposition of the surface matrix $g_s^{-1}(MM)$ of any independent film bounded by perfectly free interfaces with appropriate boundary conditions.

2.2. Interface Modes

In this section, we are interested in the interface modes localized at the boundary $z = 0$ between two semi-infinite systems. The dispersion relation derives straightforwardly as:

$$\det(g^{-1}(z, z');\ z = z' = 0) = 0 \text{ where } g^{-1}(0,0) = -(F_1 + F_2)$$

We easily obtain the equation giving the interface modes, namely:

$$F_1 + F_2 = 0 \tag{12}$$

where $F_i = \frac{\alpha_i}{\mu_i}$ $(i = 1, 2)$ for TE wave and $F_i = -\frac{\varepsilon_i}{\alpha_i}\frac{\omega^2}{c^2}$ $(i = 1, 2)$ for TM wave.

2.3. Confined Layer Modes

Now we are interested in the confined modes of a layer extending in the region $0 < z < d$ embedded between two semi-infinite systems. The response function of the system in surface space is given by:

$$g(MM) = \frac{1}{A} \begin{vmatrix} F_1 + F_2 \coth(\alpha_2 d) & \frac{F_2}{Sh(\alpha_2 d)} \\ \frac{F_2}{Sh(\alpha_2 d)} & F_1 + F_2 \coth(\alpha_2 d) \end{vmatrix} \tag{13}$$

with

$$A = F_1^2 + 2F_1F_2 \coth(\alpha_2 d) + F_2^2.$$

By setting $\det(g^{-1}(MM))$ equal to zero, one obtains the following dispersion relation:

$$(F_1^2 + F_2^2)\sinh(\alpha_2 d) + 2F_1F_2\cosh(\alpha_2 d) = 0 \tag{14}$$

2.4. Bulk Modes of Infinite Superlattice Composed of Two Alternating Layers

We shall call d_1 and d_2 the thicknesses of layers 1 and 2, respectively, with $D = d_1 + d_2$ being the period of superlattice and we assume that the z axis is along the normal to the interfaces and the wave vector component $k_{//}$, parallel to the layers, is along the x axis (see Figure 1).

The bulk Green function of system (i) is given by:

$$G_i(z, z') = -\frac{1}{2F_i}\exp[-\alpha_i\left|z - z'\right|] \tag{15}$$

and the inverse interface response function $g_i^{-1}(MM)$ of layer (i) of thickness d_i in the interface space $M \equiv \{-d_i/2, d_i/2\}$ can be written as:

$$g_i^{-1}(MM) = \begin{bmatrix} A_i & B_i \\ B_i & A_i \end{bmatrix} \tag{16}$$

where $A_i = -\frac{F_iC_i}{S_i}$, $B_i = \frac{F_i}{S_i}$, $C_i = \cosh(\alpha_i d_i)$ and $S_i = \sinh(\alpha_i d_i)$.

By the superposition of $g_{si}^{-1}(M_mM_m)$ corresponding to each layer (i), one easily obtains the Green function of superlattice in the interface space $g^{-1}(M_mM_m)$, namely written under three diagonal matrix form as:

$$g^{-1}(M_mM_m) = \begin{bmatrix} \ddots & & & & & & & & \\ & \ddots & \ddots & \ddots & & & & & \\ & & B_2 & A_2+A_1 & B_1 & & & & \\ & & & B_1 & A_1+A_2 & B_2 & & & \\ & & & & B_2 & A_2+A_1 & B_1 & & \\ & & & & & \ddots & \ddots & & \\ & & & & & & \ddots & \ddots & \\ & & & & & & & \ddots & \ddots \end{bmatrix} \tag{17}$$

The periodicity of the system enables us to introduce the Bloch wave vector k_z along the axis of the superlattice, we obtain:

$$[g(k_z, M, M)]^{-1} = \begin{pmatrix} A_1 + A_2 & B_1 + B_2e^{-ik}z^D \\ B_2e^{ik}z^D + B_1 & A_1 + A_2 \end{pmatrix} \tag{18}$$

By setting the determinant of $[g(k_z, M, M)]^{-1}$ equal to zero the dispersion relation derives straightforwardly as:

$$\cos(k_zD) = C_1C_2 + \frac{1}{2}\left(\frac{F_1}{F_2} + \frac{F_2}{F_1}\right)S_1S_2 \tag{19}$$

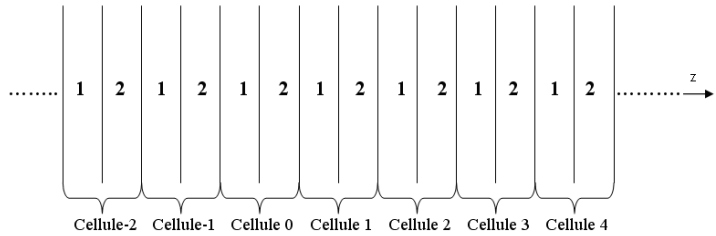

Figure 1. Diagram of infinite superlattice composed by alternating two layers.

3. NUMERICAL RESULTS AND DISCUSSION

3.1. Interface Modes

First, we are interested in the interface modes localized at the boundary $z = 0$ between a LHM and RHM. Such a wave should be exponentially decaying on both sides of the interface and, therefore, its frequency lies below the light lines of both media (i.e., both α_1 and α_2 are real, where 1 and 2 refer to the media on both sides of the interface). By taking the square in dispersion Eq. (12) we obtain:

$$\frac{\omega^2}{k_{||}^2} = \frac{\frac{\varepsilon_1}{\mu_1} - \frac{\varepsilon_2}{\mu_2}}{\frac{1}{\mu_1^2} - \frac{1_2}{\mu_2^2}} \text{ for TE modes} \quad \text{and} \quad \frac{\omega^2}{k_{||}^2} = \frac{\frac{\mu_1}{\varepsilon_1} - \frac{\mu_2}{\varepsilon_2}}{\frac{1}{\varepsilon_1^2} - \frac{1_2}{\varepsilon_2^2}} \text{ for TM modes} \quad (20)$$

One easily derives the condition for the existence of interfaces modes as follows:

For **TE modes**: either $\varepsilon_2\mu_2 < \varepsilon_1\mu_1$ and $\mu_2^2 > \mu_1^2$ or $\varepsilon_2\mu_2 > \varepsilon_1\mu_1$ and $\mu_2^2 < \mu_1^2$

For **TM modes**: either $\varepsilon_2\mu_2 < \varepsilon_1\mu_1$ and $\varepsilon_2^2 > \varepsilon_1^2$ or $\varepsilon_2\mu_2 > \varepsilon_1\mu_1$ and$\varepsilon_2^2 < \varepsilon_1^2$.

Unlike the case of an interface between two RHM, the RHM-LHM interface can support a localized mode of TE polarization. However, one can notice that the TE and TM interface modes can never exist simultaneously; i.e., the interface supports at most one localized mode of either TE or TM polarization.

3.2. Confined Modes of Layer

We consider a LHM layer of thickness d sandwiched between vacuum. Their permittivity and permeability are frequency dependent under

the following forms [17, 33–35]:

$$\varepsilon(\omega) = 1 - \frac{\omega_p^2}{\omega^2} \quad \text{and} \quad \mu(\omega) = 1 - \frac{F \times \omega^2}{\omega^2 - \omega_0^2} \tag{21}$$

where ω_0 and ω_p are the effective magnetic and electric plasma frequencies.

Let us mention that the authors of Ref. [34] have considered a multilayered structure constituting of alternating air and metamaterial slabs. These last ones are composed of metallic split ring resonators-wire metamaterial. The authors of this reference have reported how the effective parameters of the metamaterial can be derived from a microscopic structure of wire and split-resonators possessing the left-handed characteristics in the frequency ranges. The effective plasma frequency ω_p depend on the wire conductivity and the effective cross section of a wire and the skin-layer thickness, while ω_o and F depend on the inductance, resistance and capacitance of the split ring resonators wire considered. In the aim of giving different trends and emphasizing the new behaviors that can occur when varying these physical parameters, we give in what follows the evolution of the modes dispersion curves of single LHM layer and for infinite superlattice when the LHM's physical parameters are modulated.

According to the Eq. (14), in Figure 2, we show some possible behaviors of TE modes dispersion curves by choosing different parameters of the LHM layer of thickness d, the RHM medium being vacuum. The panels (1), (2) and (3) in the upper row, present the confined modes of the embedded LHM layer for different values of F (namely, $F = 0.4, 0.6$ and 0.82) with $\omega_0 = 4$ and $\omega_p = 10$. One notices the existence of many confined modes around the resonance frequency ω_0 and the transformation of the interface modes to confined modes of layer when the corresponding branches cross the light line of LHM. The panels (4), (5) and (6) in the middle row, show the confined modes of the embedded LHM layer for different values of ω_0 (namely, $\omega_0 = 3, 6$ and 8) with $F = 0.56$ and $\omega_p = 10$. One emphasizes the tendency of interference of interface modes. The examples sketched in panels (7), (8) and (9) in the lowest row, correspond to the confined modes of the embedded LHM layer for different values of ω_p (namely, $\omega_p = 5, 8$ and 12) with $F = 0.56$ and $\omega_0 = 4$.

3.3. Superlattice Constituted by Alternate Layers of LHM-RHM

Several studies of the dispersion relation and photonic band structure in superlattice constituted by alternate layers LHM-RHM in which

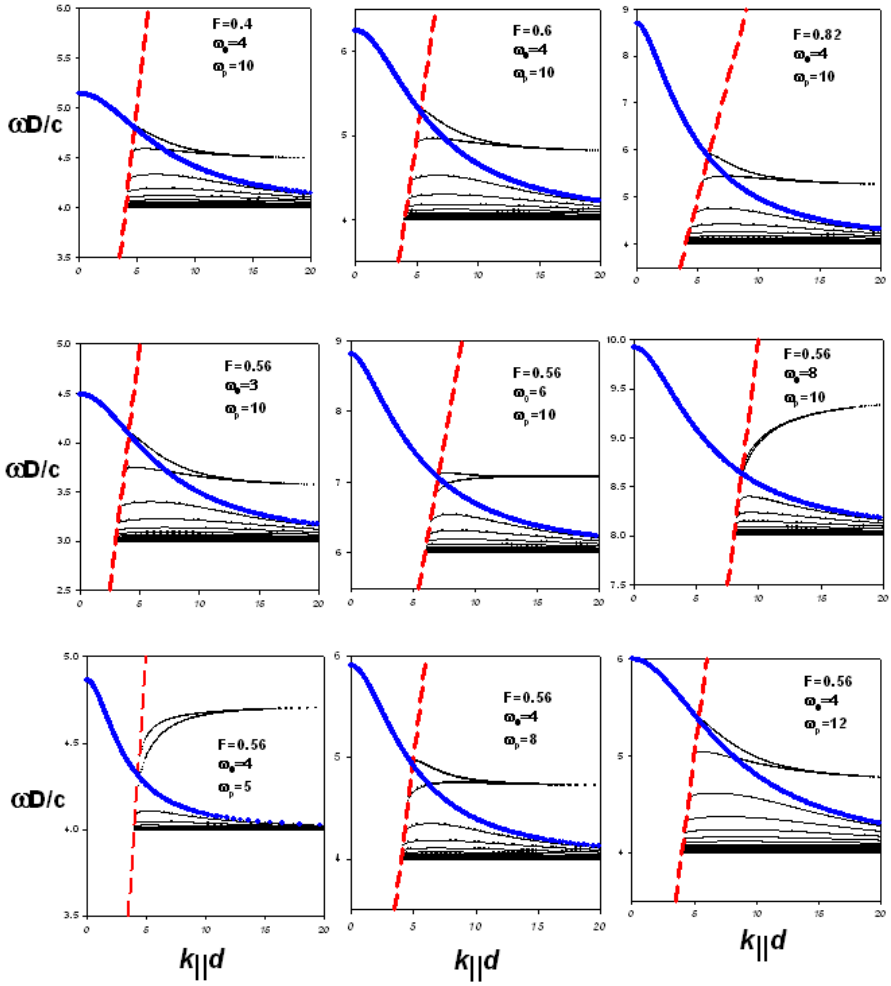

Figure 2. Dispersion curves of confined TE optical modes in LHM layer of thickness $d = 0.5D$ sandwiched between vacuum for different values of parameters F, ω_0 and ω_p. The straight lines show the light lines of vacuum (dashed line) and of the LHM layer (full line). The reduced frequency $\Omega = \omega D/c$ is presented as function of the reduced wave vector $K_{//} = k_{//}d$ parallel to the layer.

the dielectric permittivity and magnetic permeability of LHM are assumed to take constant values have been discussed. Although these parameters in LHM are in general frequency dependent, the

object in our case is to investigate the photonic band structure of one dimensional layer structures constituted by a periodical repetition of vacuum and LHM's in which the permittivity and permeability are given by (21). Assuming the possibility of realizing such LHM under the model form of layered media [21, 34], we present a detailed theoretical study of the photonic band structure of a one dimensional layered material. We investigate and discuss the band structures with various physical parameters F, ω_0 and ω_p of the LHM layer.

3.3.1. Photonic Band Structure as a Function of the Parameter F

In the following, we investigate the possible behaviors of TE and TM modes dispersion curves by choosing different values of the parameter F. The other parameters are taken to be $\omega_0 D/c = 4$ and $\omega_p D/c = 10$.

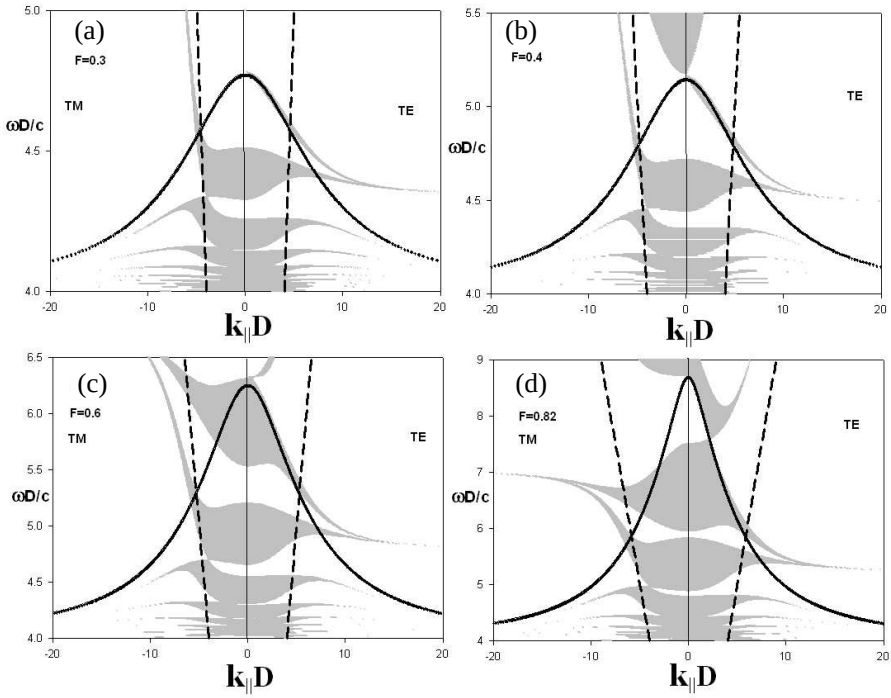

Figure 3. Projected photonic band structure of a vacuum-LHM superlattice for different values of $F = 0.3$ (a), 0.4 (b), 0.6 (c) and 0.82 (d). The filling fraction of vacuum $d_1/D = 0.5$. The straight dashed line is the vacuum light line and the heavy solid line defined by equation $\alpha_2 = 0$, separate the region of propagating and evanescent waves in LHM.

Figure 3 shows the dispersion curves $\Omega = \omega D/c$ versus $K_{//} = k_{//}D$ for $F = 0.3$ (a), 0.4 (b), 0.6 (c) and 0.82 (d). One notices the existence of narrow bands and mini-gaps in the range of frequency around the magnetic plasma frequency $\omega_0 \leq \omega \leq \frac{\omega_0}{\sqrt{1-F}}$ where the parameters of LHM, ε and μ, are simultaneously negative. These bands resulted by the interaction of confined modes in LHM layer embedded between vacuum. The novel behaviors resulting from the variation of the parameter F of the LHM is the modification of the gap frequency ranges for TE and TM polarizations. In order to have a better insight about these behaviors, we give in Figure 4 the variation of the photonic band structure Ω versus F for different values of the reduced wave vector $K_{//}$, namely $K_{//} = 0, 2, 4$ and 6, which allow us to estimate the width of the pass band and mini-gaps for given value of F.

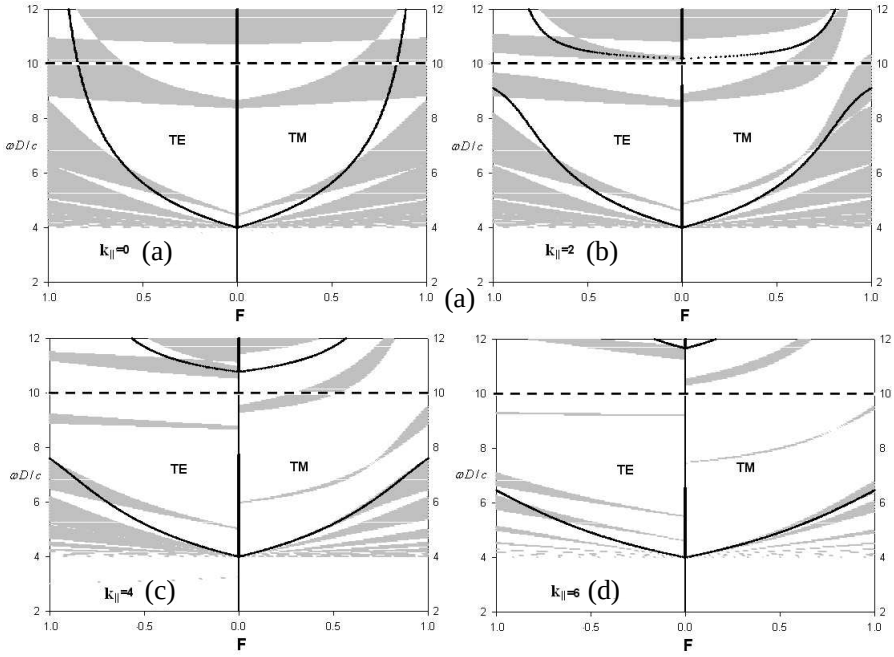

Figure 4. Variation of the photonic band structure of a vacuum-LHM superlattice versus F for different values of $K_{//} = 0.3$ (a), 0.4 (b), 0.6 (c) and 0.82 (d). The filling fraction of vacuum $d_1/D = 0.5$. The straight dashed line is the reduced electric plasma frequency $\omega_p D/c = 10$ and the heavy solid line defined by equation $\alpha_2 = 0$, separate the region of propagating and evanescent waves in LHM.

3.3.2. Photonic Band Structure as a Function of the Parameter ω_0

Now we are interested in the possible behaviors of TE and TM modes dispersion curves by choosing different values of the parameter ω_0. The other parameters are taken to be $F = 0.56$ and $\omega_p D/c = 10$. Figure 5 shows the dispersion curves Ω versus $K_{//}$ for reduced $\omega_0 D/c = 3$ (a), 6 (b), 8 (c) and 12 (d). One easily emphasizes that by increasing ω_0 we can obtain a wide pass band which gives birth to mini bands and gaps. The above result can be illustrated in Figure 6 which present the photonic band structure as the reduced frequency Ω versus ω_0 for different values of the reduced wave vector $K_{//}$, namely $K_{//} = 0, 2, 4$ and 6. Let us mention that the band photonic structures are strongly dependent on the parameter ω_0.

3.3.3. Photonic Band Structure as a Function of the Parameter ω_p

Finally, we show in Figure 7 the possible behaviors of TE and TM modes dispersion curves by choosing different values of the parameter

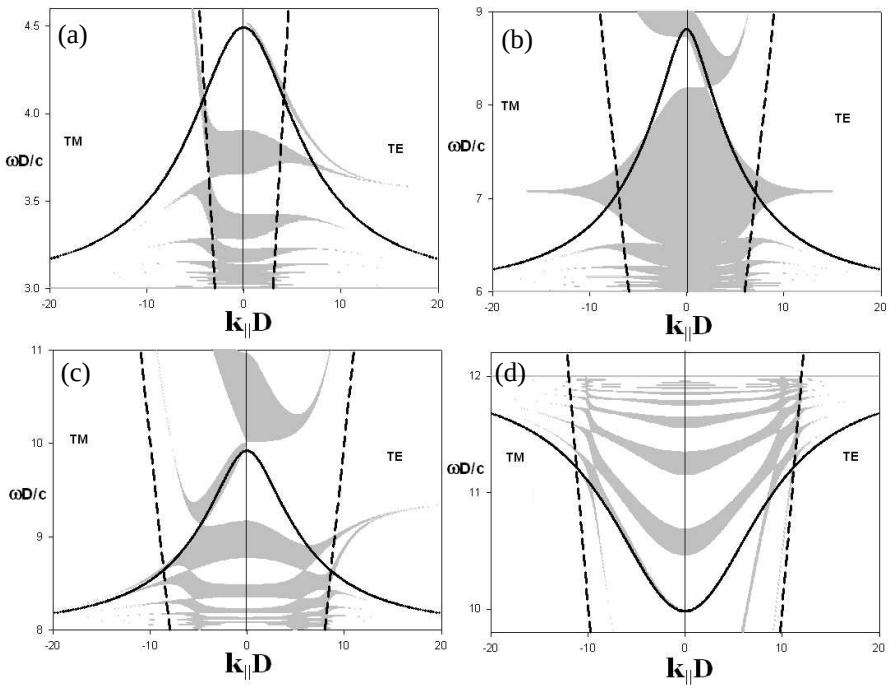

Figure 5. Same as in Figure 3 for different values of $\omega_0 D/c = 3$ (a), 6 (b), 8 (c) and 12 (d).

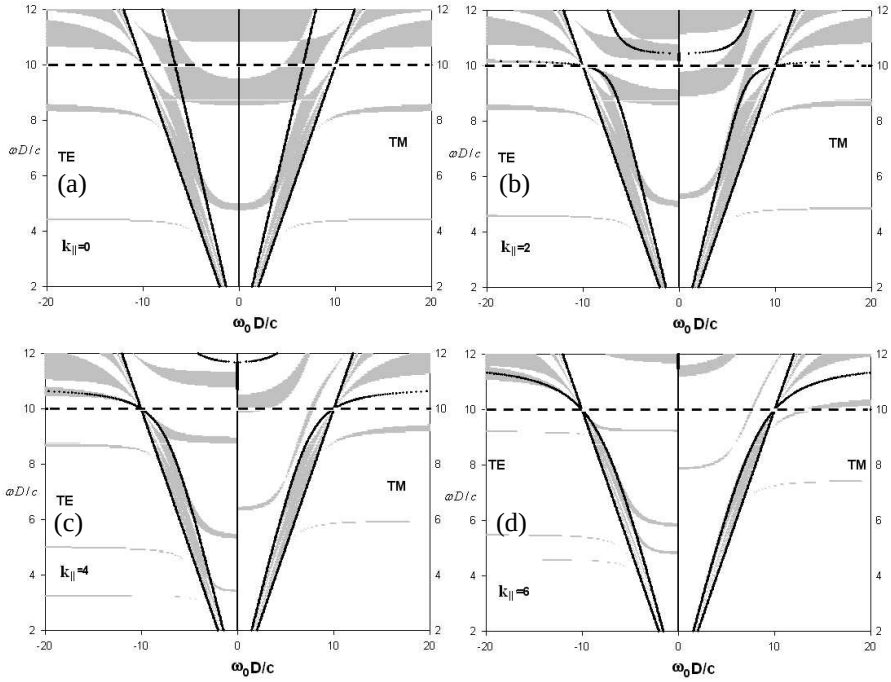

Figure 6. Variation of the photonic band structure of a vacuum-LHM superlattice versus $\omega_0 D/c$ for different values of $K_{//} = 0$ (a), 2 (b), 4 (c) and 6 (d). The filling fraction of vacuum d1/D=0.5. The heavy solid line is the light line in LHM layer. The straight dashed line is the reduced electric plasma frequency $\omega_p D/c = 10$.

ω_p with $F = 0.56$ and $\omega_0 D/c = 4$. One can recognize for both polarizations a burst of pass bands with appearance of mini-gaps for increasing ω_p.

In Figure 8, we present the variation of the reduced frequency Ω versus ω_p for different values of $k_{//}$.

4. ASSOCIATION OF TWO SUPERLATTICES

An interesting and unexpected result which is due to the presence of LHM layers is the existence in Figure 3 of an absolute band gap of TE polarization. Indeed, this frequency interval free of TE modes for any value of the wave vector $K_{//}$, depend on the physical parameter F. Consequently, a wave launched from any substrate with an arbitrary angle of incidence is prohibited from propagation and will be reflected

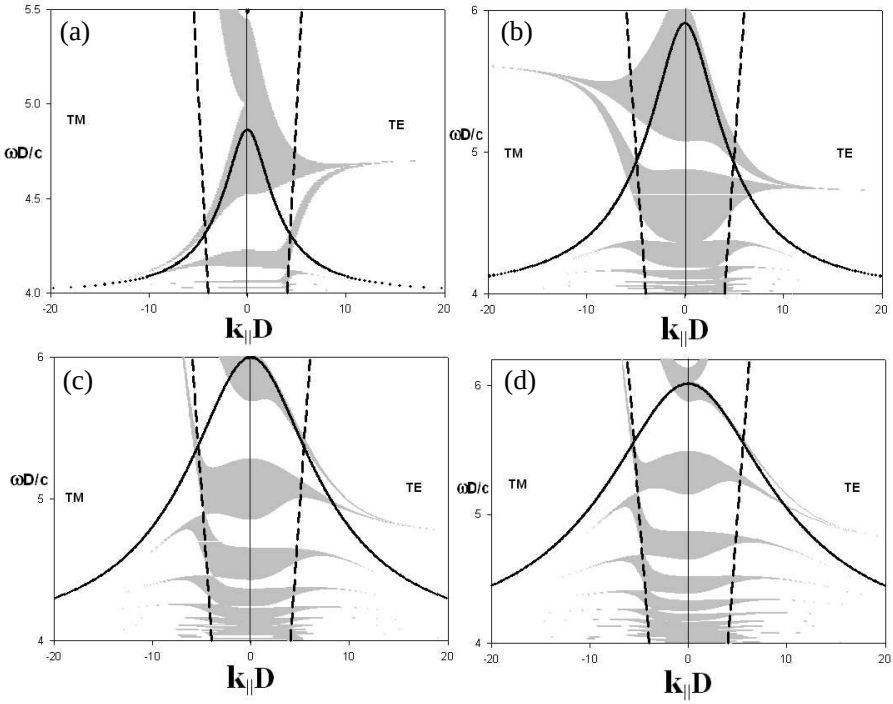

Figure 7. Same as in Figure 3 for different values of $\omega_p D/c = 5$ (a), 8 (b), 12 (c) and 15 (d).

back. The superlattice becomes a perfect mirror for TE modes, or a filter for TM modes, in this frequency range. An interesting result of Figure 5(b) is the existence of an absolute band gap of TM polarization, while such an omnidirectional gap cannot exist in ususal RHM superlattices. In these previous examples of Figures 3 and 5, we have shown that an appropriate choice of the material parameters and the LHM/RHM superlattice can display an omnidirectional gap for either TE or TM polarization. In the following, we propose another kind of structure to create complete gap for both wave polarizations in the one dimensional photonic crystal by the association of two superlattices composed by LHM-RHM. For the sake of briefness in this paper, we choose vacuum as the RHM and the other parameters are taken to be:

First superlattice:

$$LHM \begin{cases} \varepsilon_2(\omega) = 1 - \frac{\omega_{p2}^2}{\omega^2} \\ \mu_2(\omega) = 1 - \frac{F_2 \times \omega^2}{\omega^2 - \omega_{02}^2} \end{cases}$$

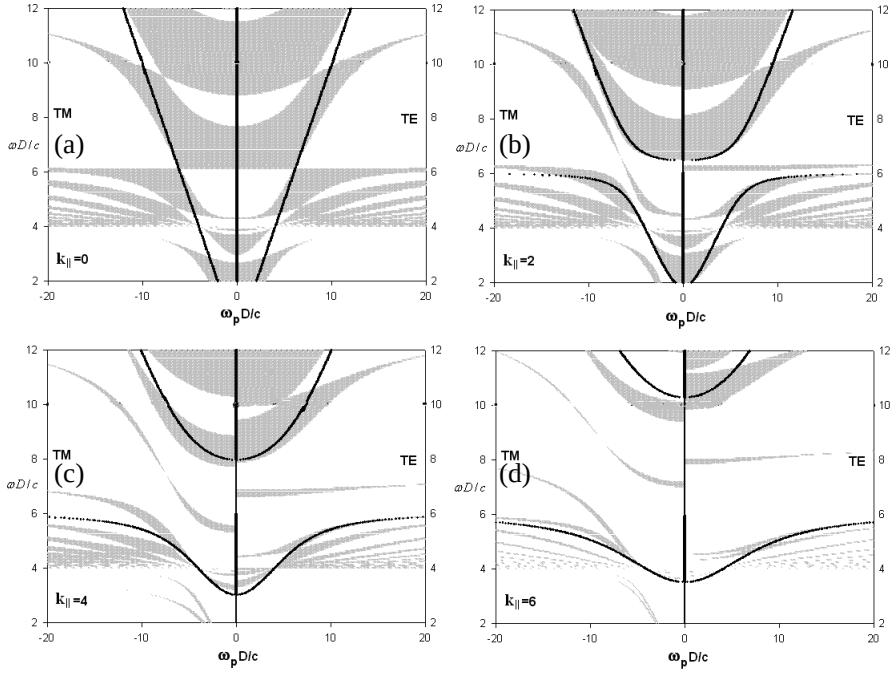

Figure 8. Varaitaion of the photonic band structure of a vacuum-LHM superlattice versus $\omega_p D/c$ for different values of $K_{//} = 0$ (a), 2 (b), 4 (c) and 6 (d). The filling fraction of vacuum $d_1/D = 0.5$. The heavy solid line is the light line in LHM layer.

where $F_2 = 0.56, \omega_{02}D/c = 7.6, \omega_{P2}D/c = 10$ and $d_1 = d_2 = D/2$.

Second superlattice:

$$LHM \begin{cases} \varepsilon_4(\omega) = 1 - \frac{\omega_{p4}^2}{\omega^2} \\ \mu_4(\omega) = 1 - \frac{F_4 \times \omega^2}{\omega^2 - \omega_{04}^2} \end{cases}$$

where $F_4 = 0.75, \omega_{04}D/c = 4, \omega_{P4}D/c = 10, d_1 = 0.6D$ and $d_2 = 0.4D$.

The projected photonic band structures for each superlattice are sketched in Figures 9 and 10, respectively. The shaded and white areas correspond to the pass bands and the gaps of suprelattice.

Considering the effect that only the wave setting simultaneously in the pass bands of each superlattice can be propagated through the composite system, in Figure 11, we show the behaviors of TE modes (right side) and TM modes (left side) dispersion curves corresponding to the superposition of two superlattices.

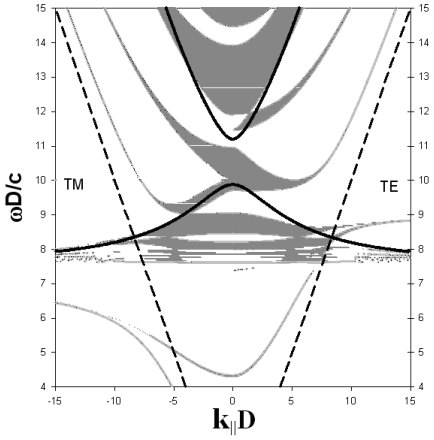

Figure 9. Photonic band structure of the first vacuum-LHM infinite superlattice. $d_1 = d_2 = D/2$, $F_2 = 0.56$, $\omega_{02}D/c = 7.6$ and $\omega_{p2}D/c = 10$. The straight dashed line is the vacuum light line and the heavy solid line is the light line of LHM layer.

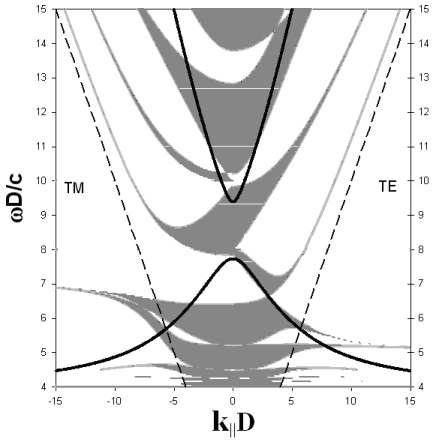

Figure 10. Photonic band structure of the second vacuum-LHM infinite superlattice. $d_1 = 0.6D$, $d_2 = 0.4D$, $F_4 = 0.75$, $\omega_{04}D/c = 4$ and $\omega_{p4}D/c = 10$. The straight dashed line is the vacuum light line and the heavy solid line is the light line of LHM layer.

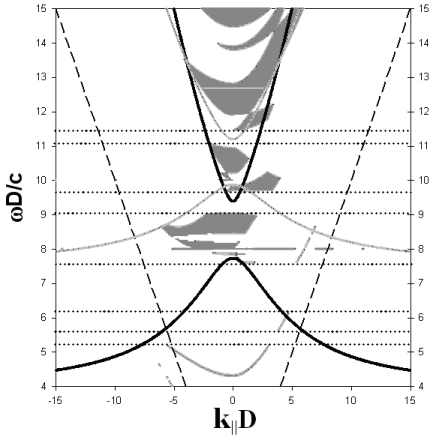

Figure 11. Superposition of the projected photonic band structure of two superlattices sketched in Fig. 9 and Fig. 10. The grey and the black heavy solid lines are, respectively, the light lines in superlattices 1 et 2. The dashed straight lines show the widths of the gaps.

An interesting result which is due to the association of two types of Vacuum-LHM superlattice is the appearance of three absolute gaps setting, respectively in frequency range: $6.3 \leq \omega D/c \leq 7.7$, $9 \leq \omega D/c \leq 9.6$ and $11.05 \leq \omega D/c \leq 11.5$.

We emphasize that an appropriate choice of thickness of layers from which the two superlattices are constructed allows us to obtain a wide absolute gap for both wave polarizations in the way that the gaps of each superlattice annihilate the pass band setting in the same frequency range of the other superlattice. Therefore, it should be possible to realize in a certain frequency range an omnidirectional reflector of light for both polarizations.

5. CONCLUSION

In this contribution, we have successfully applied the theory of Green's function method to determine the response functions $\overleftrightarrow{G}_i(\omega/\vec{x}, \vec{x}')$, $\overleftrightarrow{g}_s(\omega/\vec{x}, \vec{x}')$, $g(z, z')$, $g(MM)$ and $g(k_z, M, M)$ for infinite, semi-infinite system, interface between two semi-infinite systems, layer and superlattice, respectively. Therefore, by using the dispersion relation associated to each case, we have sketched the behaviors of TE and TM modes dispersion curves by choosing different parameters of LHM, more particularly where the dielectric permittivity and magnetic permeability are frequency dependent in each layer. We have also illustrated the behaviors of the photonic band structure for different values of parameters (F, ω_0, ω_p) which describe the permittivity and the permeability of dispersive LHM. In particular, we have emphasized that the novel behavior resulting from the variation of the parameter F, tied to the magnetic permeability of LHM, is the modification of the gap frequency ranges for TE and TM polarizations. We have shown that the band photonic structure strongly depends on the parameters ω_p and ω_0. Finally, a new phenomenon associated with the presence of the LHM is the possibility of absolute band gaps, of either TE or TM polarization, when the material parameters are chosen appropriately. This enables us to propose an application of our structure for realizing an omnidirectional optical mirror that prevents propagation of optical waves of TE and TM polarizations for a given frequency range. Combination in tandem of two such multilayers can yield an omnidirectional reflector of light for both polarizations.

ACKNOWLEDGMENT

D. Bria gratefully acknowledges the hospitality of Abdus Salam International Centre for theoretical Physics, Trieste, Italy, where a part of this work was done within the framework of the Associateship Scheme. We thank Prof. A. Mazari for his very critical comments to improve the English and the form of this article.

REFERENCES

1. Pendry, J. B., "Photonic crystals and light localization in the 21th century," *NATO Science*, C. M. Soukoulis (ed.), Series C, Vol. 563 of (Kluwer, Dordrecht 2002), 329, 2002.
2. Veselago, V. G., "The electrodynamics of substances with simultaneously negative values of permittivity and permeability," *Sov. Phys. Usp.*, Vol. 10, 509, 1968.
3. Shelby, R. A., D. R. Smith, and S. Schultz, "Experimental verification of a negative index of refraction," *Science*, Vol. 292, 77, 2001.
4. Marqués, R., J. Martel, F. Mesa, and F. Medina, "Left-handed-media simulation and transmission of EM waves in subwavelength split-ring-resonator-loaded metallic waveguides," *Phys. Rev. Lett.*, Vol. 89, 138901, 2002.
5. Pendry, J. B., A. J. Holden, D. J. Robbins, and W. J. Steweat, "Magnetism from conductors and enhanced nonlinear phenomena," *IEEE Transactions on Microwaves and Techniques*, Vol. 47, 2075, 2000.
6. Foteinoupoulou, S., E. N. Economou, and C. M. Soukoulis, "Refraction in media with a negative refractive index," *Phys. Rev. Lett.*, Vol. 90, 107402, 2003.
7. Houck, A. A., J. B. Brock, and I. L. Chuang, "Experimental observations of a left-handed material that obeys Snell's law," *Phys. Rev. Lett.*, Vol. 90, 137401, 2003.
8. Parazzoli, C. G., R. B. Greegor, K. Li, B. E. C. Koltenbah, and M. Tanielian, "Experimental verification and simulation of negative index of refraction using Snell's law," *Phys. Rev. Lett.*, Vol. 90, 107401, 2003.
9. Ziolkowski, R. W. and E. Heyman, "Wave propagation in media having negative permittivity and permeability," *Phys. Rev. E*, Vol. 64, 056625, 2001.
10. Smith, D. R., D. Schurig, and J. B. Pendry, "Electromagnetic

wave propagation in media with indefinite permittivity and permeability tensors," *Appl. Phys. Lett.*, Vol. 81, 2713, 2002.

11. Pendry, J. B., "Negative refraction makes a perfect lens," *Phys. Rev. Lett.*, Vol. 85, 3966, 2000.
12. Feise, M. W., P. J. Bevelacqua, and J. B. Schneider, "Effects of surface waves on the behaviour of perfect lenses," *Phys. Rev. B*, Vol. 66, 035113, 2002.
13. Fang, N. and X. Zhang, "Imaging properties of a metamaterial superlens," *Appl. Phys. Lett.*, Vol. 82, 161, 2003.
14. Zhang, Z. M. and C. J. Fu, "Unusual photon tunnelling in the presence of a layer with a negative refractive index," *Appl. Phys. Lett.*, Vol. 80, 1097, 2002.
15. Enoch, S., G. Tayeb, P. Sabourous, N. Guérin, and P. Vincent, "A metamaterial for directive emission," *Phys. Rev. Lett.*, Vol. 89, 213902, 2002.
16. Nefedov, I. S. and S. A. Tretyakov, "Photonic band gap structure containing metamaterial with negative permittivity and permeability," *Phys. Rev. E*, Vol. 66, 036611, 2002.
17. Li, J., L. Zhou, C. T. Chan, and P. Sheng, "Photonic band gap from a stack of positive and negative index materials," *Phys. Rev. Lett.*, Vol. 90, 083901, 2003.
18. Bria, D., B. Djafari-Rouhani, A. Akjouj, L. Dobrzynski, J. P. Vigneron, E. H. ElBoudouti, and A. Nougaoui, "Band structure and omnidirectional photonic band gap in lamellar structures with left-handed materials," *Phys. Rev. E*, Vol. 69, 066613, 2004.
19. Wu, L., S. He, and L. Shen, "Band structure for a one-dimensional photonic crystal containing left-handed materials," *Phys. Rev. B*, Vol. 67, 235103, 2003.
20. Xiang, Y., X. Dai, and S. Wen, "Omnodirectional gaps of one-dimensional potonic crystals containing indefinite metamaterials," *J. Opt. Soc. Am. B*, Vol. 24, 2033, 2010.
21. Zhang, F., D. P. Gaillot, C. Croënne, E. Lheurette, X. Mélique, and D. Lippens, "Low-loss left-anded metamaterials at millimeter waves," *Appl. Phys. Let.*, Vol. 93, 083104, 2008.
22. Xinag, Y., X. Dai, S. Wen, and D. Fan, "Properties of omnidirectional gap and defect mode of one-dimensionla photonic crystal containing indefinite metamaterials with hyperbolic dispersion," *J. Appl. Phys.*, Vol. 102, 093107, 2007.
23. Sun, W.-H., Y. Lu, R.-W. Peng, L.-S. Cao, D. Li, X. Wu, and M. Wang, "Omnidirectional transparency induced by matched

impedance disordered metamaterials," *J. Appl. Phys.*, Vol. 106, 013104, 2009.

24. De Dios-Leyva, M. and J. C. Drake-Pérez, "Zero-width band gap associated with the $n = 0$ condition in photonic crystals containing left-handed materials," *Phys. Rev. E*, Vol. 79, 036608, 2009.
25. Fink, J. N., S. Winn, S. Fan, C. Chen, J. Michel, J. D. Joannopoulos, and E. L. Thomas, "Dielectric omnidirectional reflector," *Science*, Vol. 282, 1679, 1998.
26. Dowling, J. P., "Mirror on the wall: You're omnidirectional after all?" *Science*, Vol. 282, 1841, 1998.
27. Bria, D., B. Djafari-Rouhani, E. H. El Boudouti, A. Mir, A. Akjouj, and A. Nougaoui, "Omnidirectional optical mirror in a cladded-superlattice structure," *J. Appl. Phys.*, Vol. 91, 2569, 2002.
28. Bria, D. and B. Djafari-Rouhani, "Omnidirectional elastic band gap in finite lamellar structures," *Phys. Rev. E*, Vol. 66, 056609, 2002.
29. Xiang, Y., L. Ran, J. T. Huangfu, H. S. Chen, and J. A. Kong, "Experimental verification of zero order bandgap in a layered stack of left-handed and right-handed materials," *Opt. Express*, Vol. 14, 2223, 2006.
30. Aylo, R., P. P. Banerjee, and G. Nehmetallah, "Perturbed multilayered structures of positive and negative index materials," *J. Opt. Soc. Am. B*, Vol. 27, 599, 2010.
31. Dobrzynski, L., "Interface response theory of continuous composite materials," *Surf. Sci.*, Vol. 180, 489, 1987.
32. Ouchani, N., D. Bria, B. Djafari-Rouhani, and A. Nougaoui, "Transverse-electric/Transversemagnetic polarization converter using 1D finite biaxial photonic crystal," *J. Opt. Soc. Am. A*, Vol. 24, No. 9, 2710, 2007.
33. Ruppin, R., "Surface polaritons of a left-handed material slab," *J. Phys. Condens. Matter*, Vol. 13, 1811, 2001.
34. Shadrivov, I. V., N. A. Zharova, A. A. Zharov, and Y. S. Kivshar, "Defect modes and transmission properties of left-handed bandgaps structures," *Phys. Rev. E*, Vol. 70, 046615, 2004.
35. Cocoletzi, G. H., L. Dobrzynski, B. Djafari-Rouhani, H. Al-Wahsh, and D. Bria, "Electromagnetic wave propagation in quasi-one-dimensional comb-like structures made up of dissipative negative-phase-velocity materials," *J. Phys.: Condens. Matter*, Vol. 18, 3683, 2006.